LETTER

doi:10.1038/nature22372

uORF-mediated translation allows engineered plant disease resistance without fitness costs

Guoyong Xu[1]*, Meng Yuan[2]*, Chaoren Ai[2], Lijing Liu[1], Edward Zhuang[1], Sargis Karapetyan[1], Shiping Wang[2] & Xinnian Dong[1]

Controlling plant disease has been a struggle for humankind since the advent of agriculture. Studies of plant immune mechanisms have led to strategies of engineering resistant crops through ectopic transcription of plants' own defence genes, such as the master immune regulatory gene *NPR1* (ref. 1). However, enhanced resistance obtained through such strategies is often associated with substantial penalties to fitness[2], making the resulting products undesirable for agricultural applications. To remedy this problem, we sought more stringent mechanisms of expressing defence proteins. On the basis of our latest finding that translation of key immune regulators, such as TBF1 (ref. 3), is rapidly and transiently induced upon pathogen challenge (see accompanying paper[4]), we developed a 'TBF1-cassette' consisting of not only the immune-inducible promoter but also two pathogen-responsive upstream open reading frames (uORFs$_{TBF1}$) of the *TBF1* gene. Here we demonstrate that inclusion of uORFs$_{TBF1}$-mediated translational control over the production of snc1-1 (an autoactivated immune receptor) in *Arabidopsis thaliana* and *At*NPR1 in rice enables us to engineer broad-spectrum disease resistance without compromising plant fitness in the laboratory or in the field. This broadly applicable strategy may lead to decreased pesticide use and reduce the selective pressure for resistant pathogens.

To meet the demand for food production caused by the rapid expansion of world population while limiting the use of pesticides, which are potential pollutants, new strategies must be developed to control crop diseases. As an alternative to traditional chemical and breeding methods, studies of plant immune mechanisms have made it possible to engineer resistance through ectopic expression of plants' own resistance-conferring genes[5]. The first line of active defence in plants involves recognition of microbial/damage-associated molecular patterns (M/DAMPs) by host pattern-recognizing receptors (PRRs) in pattern-triggered immunity (PTI)[6]. Ectopic expression of PRRs for MAMPs[7,8] and the DAMP signal eATP[9], as well as *in vivo* release of the DAMP molecules, oligogalacturonides[10], have all been shown to enhance resistance in transgenic plants. Besides PRR-mediated basal resistance, plant genomes encode hundreds of intracellular nucleotide-binding and leucine-rich repeat immune receptors (also known as 'R proteins') to detect the presence of pathogen effectors delivered inside plant cells[11]. Individual or stacked R genes have been transformed into plants to confer effector-triggered immunity[12,13]. In addition to PRR and R genes, *NPR1* is another favourite gene used in engineering plant resistance[5]. Unlike immune receptors that are activated by specific MAMPs and pathogen effectors, NPR1 is a positive regulator of broad-spectrum resistance induced by a general plant immune signal, salicylic acid[1]. Overexpression of *Arabidopsis* NPR1 (*At*NPR1) could enhance resistance against a variety of pathogens in diverse plant families such as rice[14–16].

A major challenge in engineering disease resistance, however, is to overcome the associated fitness costs[2]. In the absence of specialized immune cells, immune induction in plants involves switching from growth-related activities to defence[3,17]. Plants normally avoid autoimmunity by tightly controlling transcription, messenger RNA (mRNA) nuclear export, and degradation of defence proteins[18]. However, only transcriptional control has been used prevalently so far in engineering disease resistance[2]. On the basis of our global translatome analysis[4], we discovered translation to be a fundamental layer of regulation during immune induction, which can be explored to allow more stringent pathogen-inducible expression of defence proteins.

To test our hypothesis that tighter control of defence protein translation can minimize the fitness penalties associated with enhanced disease resistance, we used the *TBF1* promoter (TBF1p) and the 5′ leader sequence (before the start codon for TBF1), which we designated as the 'TBF1-cassette'. TBF1 is an important transcription factor for the growth-to-defence switch upon immune induction. Translation of TBF1 is normally suppressed by two uORFs within the 5′ leader sequence[3]. BLAST analysis showed that uORF2$_{TBF1}$, the major mRNA feature conferring the translational suppression[3,4]), is conserved across plant species (>50% identity) (Extended Data Fig. 1), suggesting an evolutionarily conserved control mechanism and a potential use of TBF1-cassette to regulate defence protein production in plant species other than *Arabidopsis*.

To explore the application of uORFs$_{TBF1}$, we first demonstrated its capacity to control both cytosol- and endoplasmic reticulum (ER)-synthesized proteins ('Target') using firefly luciferase (LUC; Extended Data Fig. 2a) and green fluorescent protein (GFP$_{ER}$; Extended Data Fig. 2b), respectively, as proxies through transient expression in *Nicotiana benthamiana* (Fig. 1a–c and Extended Data Fig. 2c, d). This uORFs$_{TBF1}$-mediated translational suppression was strong enough to prevent cell death induced by overexpression of TBF1 (TBF1–YFP, TBF1 fused with yellow fluorescent protein) observed in *35S:uorfs$_{TBF1}$-TBF1–YFP* (Fig. 1d and Extended Data Fig. 2e). Similar repression activity was observed for uORF2b$_{bZIP11}$ of the sucrose-responsive *bZIP11* gene[19] (Extended Data Fig. 2f–l). However, unlike uORFs$_{TBF1}$, the uORF2$_{bZIP11}$-mediated repression could not be alleviated by the MAMP signal elf18 (Extended Data Fig. 2m, n). These results support the potential utility of uORFs$_{TBF1}$ in providing stringent control of cytosol- and ER-synthesized defence proteins specifically for engineering disease resistance.

To monitor the effect of uORFs$_{TBF1}$ on translational efficiency, a dual-luciferase system was constructed to calculate the ratio of LUC activity to the control renilla luciferase (RLUC) activity (Fig. 1e). The resulting transgenic plants were tested for responsiveness to bacterial pathogens *Pseudomonas syringae* pathovar (pv.) *maculicola* ES4326 (*Psm* ES4326), *Pseudomonas* pv. *tomato* (*Pst*) DC3000, and the corresponding mutant of the type III secretion system *Pst* DC3000 *hrcC*$^{-}$, as well as to MAMP signals, elf18, and flg22. The equally rapid induction in the reporter translational efficiency by all treatments suggests that it is probably a part of pattern-triggered immunity, which does not

[1]Howard Hughes Medical Institute-Gordon and Betty Moore Foundation, Department of Biology, Duke University, Durham, North Carolina 27708, USA. [2]National Key Laboratory of Crop Genetic Improvement, National Centre of Plant Gene Research (Wuhan), Huazhong Agricultural University, 430070 Wuhan, China.
*These authors contributed equally to this work.

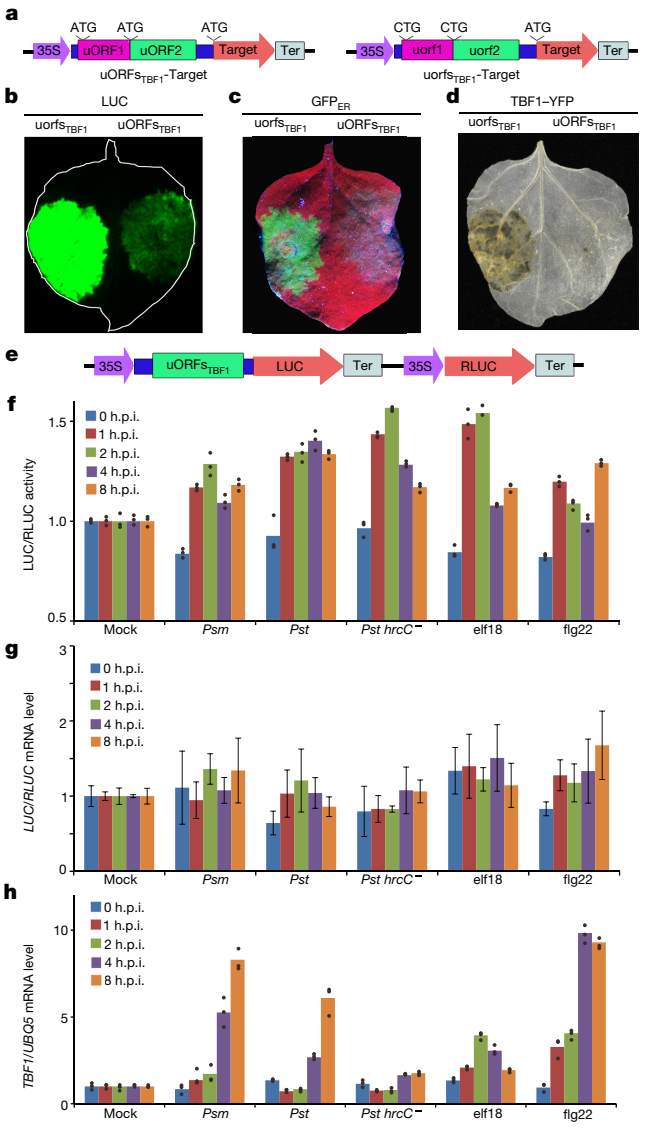

Figure 1 | uORFs$_{TBF1}$-mediated translational and TBF1 promoter-mediated transcriptional regulation. a, Schematics of WT uORFs$_{TBF1}$ or mutant uorfs$_{TBF1}$. **b**–**d**, LUC activity (**b**), GFP$_{ER}$ fluorescence (**c**), and cell death induced by TBF1–YFP (**d**), representative of six images. **e**, Dual-luciferase system. **f**, Translational changes of the reporter to different treatments. Mean of the LUC/RLUC activity ratios normalized to mock ($n = 3$). **g**, *LUC/RLUC* mRNA levels in **f**. Mean ± s.d. of *LUC/RLUC* mRNA normalized to mock ($n = 6$). **h**, Endogenous *TBF1* mRNA levels ($n = 3$). *UBQ5*, internal control. Solid circles, individual biological replicates. See Extended Data Fig. 2.

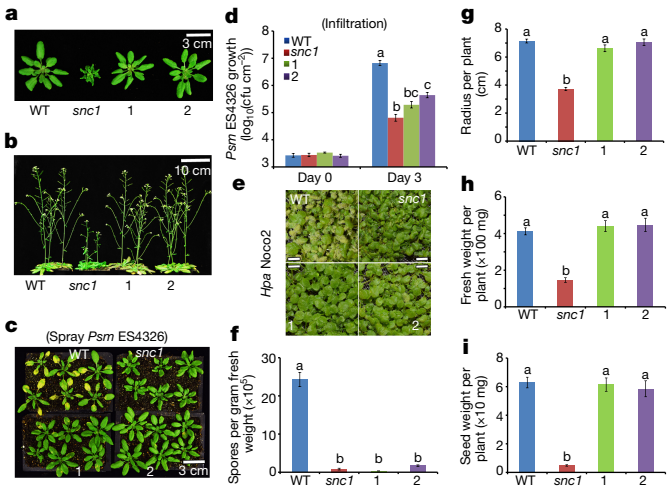

Figure 2 | Effects of controlling transcription and translation of *snc1* in *Arabidopsis*. a, **b**, Effects on vegetative and reproductive growth; *snc1*, autoactivated mutant; numbers 1 and 2, independent lines carrying *TBF1p:uORFs$_{TBF1}$-snc1*. Representative of five images. **c**, **d**, *Psm* ES4326 growth after inoculation by spray (**c**) or infiltration (**d**). **e**, **f**, Photographs (representative of six images; scale bar, 0.5 cm) and quantification of *Hpa* Noco2. **g**–**i**, Rosette radius, fresh weight, and total seed weight. Mean ± s.e.m. Different letters above bars indicate significant differences ($P < 0.05$). See Source Data for sample size (n) and Extended Data Fig. 4 for two additional lines.

involve bacterial type III effectors (Fig. 1f). The transient increases in translation were not correlated with significant changes in mRNA levels (Fig. 1g). In parallel, the endogenous *TBF1* mRNA level was elevated at later time points than the translational increases observed using the reporter (Fig. 1h), suggesting that in response to pathogen challenge, translational induction may precede transcriptional reprogramming in plants.

To engineer resistant plants using TBF1-cassette we picked two candidates from *Arabidopsis*, snc1-1 (ref. 20) and NPR1 (ref. 14). The *Arabidopsis* snc1-1 (for simplicity, snc1 from here on) is an autoactivated point mutant of the nucleotide-binding and leucine-rich repeat immune receptor SNC1. Even though the *snc1* mutant plants have constitutively elevated resistance to various pathogens, their growth is significantly retarded[20]. Such a growth defect is also prevalent in transgenic plants ectopically expressing the wild-type (WT) *SNC1* by either the 35S promoter or its native promoter[21,22], limiting the utility of *SNC1*, and perhaps other *R* genes, in engineering resistant plants. To overcome the fitness penalty associated with the snc1 mutant, we put it under the control of uORFs$_{TBF1}$ driven by either the 35S promoter or TBF1p to create *35S:uORFs$_{TBF1}$-snc1* and *TBF1p:uORFs$_{TBF1}$-snc1*, respectively. As controls, we also generated *35S:uorfs$_{TBF1}$-snc1* and *TBF1p:uorfs$_{TBF1}$-snc1*, in which the start codons of the uORFs were mutated. The first generation of transgenic *Arabidopsis* (T_1) with these four constructs displayed three distinct developmental phenotypes: type I plants were small in rosette diameter, dwarf, and exhibited chlorosis; type II plants were healthier but still dwarf; and type III plants were indistinguishable from WT (Extended Data Fig. 3). We found that regulating either transcription or translation of *snc1* markedly improved plant growth, as judged by the increased percentage of type III plants. The highest percentage of type III plants was found in *TBF1p:uORFs$_{TBF1}$-snc1* transformants, in which *snc1* was regulated by TBF1-cassette at both transcriptional and translational levels. The absence of type I plants in these transformants clearly demonstrated the stringency of TBF1-cassette (Extended Data Fig. 3).

We propagated the transformants to obtain homozygotes for the transgene. For the *TBF1p:uorfs$_{TBF1}$-snc1* and *35S:uORFs$_{TBF1}$-snc1* lines, homozygosity caused most of the type III plants in T_1 to show the type II phenotype in T_2. But for *TBF1p:uORFs$_{TBF1}$-snc1* transformants, they maintained their normal growth phenotype as homozygotes. We then picked four independent *TBF1p:uORFs$_{TBF1}$-snc1* lines for further disease resistance and fitness tests (Fig. 2a, b). We first showed that these transgenic lines indeed had elevated resistance to *Psm* ES4326 by either spray inoculation or infiltration (Fig. 2c, d and Extended Data Fig. 4a, b). They also displayed enhanced resistance to *Hyaloperonospora arabidopsidis* Noco2 (*Hpa* Noco2), an oomycete pathogen which causes downy mildew in *Arabidopsis* (Fig. 2e, f and Extended Data Fig. 4c). However, in contrast to *snc1*, these transgenic lines showed almost the same fitness as WT, including total seed weight per plant (Fig. 2g–i and Extended Data Fig. 4d–g). Upon *Psm* ES4326 challenge, we detected significant increases in the snc1 protein within 2 hours post infection (h.p.i.) in all four *TBF1p:uORFs$_{TBF1}$-snc1* transgenic lines, but not in WT or *snc1* (Extended Data Fig. 4h, i). These data provide a proof of concept that adding pathogen-inducible

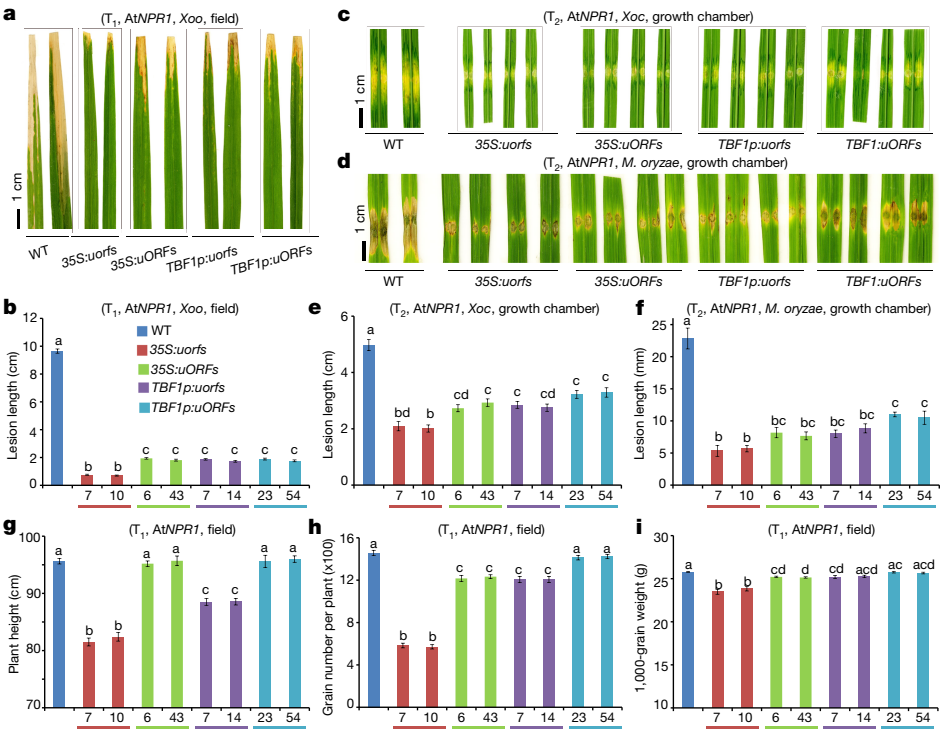

Figure 3 | Effects of controlling transcription and translation of At*NPR1* in rice. a, **b**, Symptoms and quantification after *Xoo* inoculation in field-grown T_1 plants. Individual plant numbers are given below the *x* axis. **c**–**f**, Symptoms and quantification after *Xoc* (**c**, **e**, water-soaking) and *M. oryzae* (**d**, **f**) in T_2 plants. **g**–**i**, Fitness under field conditions, including plant height (**g**), the number of grains per plant (**h**), and 1,000-grain weight (**i**). Mean ± s.e.m. Different letters above bars indicate significant differences ($P < 0.05$). See Source Data for sample size (*n*) and Extended Data Figs 7 and 8 for data from two additional lines and for more fitness parameters.

translational control is an effective way to enhance plant resistance without fitness costs.

We next applied TBF1-cassette to engineering resistance in rice, which is one of the most important staple crops in the world. Using *35S:uORFs$_{TBF1}$-LUC* and *35S:uorfs$_{TBF1}$-LUC* (Fig. 1b), we first showed that the *Arabidopsis* uORFs$_{TBF1}$ could suppress translation without significantly influencing mRNA levels in the rice (*Oryza sativa*) cultivar ZH11 (Extended Data Fig. 5a, b). We then chose At*NPR1* (ref. 1), which has been shown to confer broad-spectrum disease resistance in a variety of plants, as the transgene. However, it is known that overexpressing At*NPR1* in rice by the maize ubiquitin promoter causes growth retardation, seed size reduction, and development of the so-called lesion mimic disease phenotype under certain environmental conditions[15,23]. To remedy the fitness problem, we expressed the At*NPR1–EGFP* fusion gene under the following four regulatory systems: *35S:uorfs$_{TBF1}$*-At*NPR1–EGFP*, *35S:uORFs$_{TBF1}$*-At*NPR1–EGFP*, *TBF1p:uorfs$_{TBF1}$*-At*NPR1–EGFP*, and *TBF1p:uORFs$_{TBF1}$*-At*NPR1–EGFP*. These four constructs were assigned different codes for blind testing of resistance and fitness phenotypes. Under growth chamber conditions, either the TBF1p-mediated transcriptional or the uORFs$_{TBF1}$-mediated translational control largely decreased the ratio and the severity of rice plants with lesion mimic disease (Extended Data Fig. 5c). However, the best results were obtained using TBF1-cassette with both transcriptional and translational control. Next, we tested plant resistance to the bacterial pathogen *Xanthomonas oryzae* pv. *oryzae* (*Xoo*), the causal agent for rice blight, in the first (T_0 in rice research) and the second (T_1) generations of transformants under the greenhouse conditions where lesion mimic disease was not observed even for *35S:uorfs$_{TBF1}$*-At*NPR1*. Unsurprisingly, the *35S:uorfs$_{TBF1}$*-At*NPR1* plants displayed the highest level of resistance to *Xoo*, owing to the constitutive transcription and translation of At*NPR1* (Extended Data Figs 6 and 7a, b). However, similar levels of resistance were also observed in plants with either transcriptional or translational control or with both. Notably, these resistance results were faithfully reproduced in the field (Fig. 3a, b and Extended Data Fig. 7c). In response to *Xoo* challenge, transgenic lines with functional uORFs$_{TBF1}$ displayed transient *At*NPR1 protein increases, which peaked around 2 h.p.i., even in the absence of significant changes in mRNA levels (for example, *35S:uORFs$_{TBF1}$*-At*NPR1* in Extended Data Fig. 7d, e).

To determine the spectrum of *At*NPR1-mediated resistance, we inoculated the third generation of transgenic rice plants (T_2) with *X. oryzae* pv. *oryzicola* (*Xoc*) and *Magnaporthe oryzae* (*M. oryzae*), the causal pathogens for rice bacterial leaf streak and fungal blast, respectively. We observed similar patterns of enhanced resistance against *Xoc* and *M. oryzae* in growth chambers designated for these controlled pathogens (Fig. 3c–f) as for *Xoo*, confirming the broad spectrum of *At*NPR1-mediated resistance. The lack of significant variation among the different transgenic lines suggests that they all had saturating levels of *At*NPR1 in conferring resistance.

We then performed detailed fitness tests on these transgenic plants in the field and found that constitutive transcription and translation of At*NPR1* in *35S:uorfs$_{TBF1}$*-At*NPR1* plants clearly had fitness penalties (Fig. 3g–i and Extended Data Fig. 8). Addition of transcriptional or/and translational control of At*NPR1* significantly reduced costs to agronomically important traits, with a combination of both transcriptional and translational control performing the best in eliminating cost on yield on the basis of the number of grains per plant and 1,000-grain weight (Fig. 3h, i).

Using TBF1-cassette, we established a new strategy of enhancing broad-spectrum disease resistance with minimal adverse effects on plant growth and development. The ubiquitous presence of uORFs in mRNAs of organisms ranging from yeast (13% of all mRNA)[24] to humans (49% of all mRNA)[25] suggests the potentially broad utility of these mRNA features for the precise control of transgene expression.

Online Content Methods, along with any additional Extended Data display items and Source Data, are available in the online version of the paper; references unique to these sections appear only in the online paper.

Received 8 September 2016; accepted 19 April 2017.
Published online 17 May 2017.

1. Fu, Z. Q. & Dong, X. Systemic acquired resistance: turning local infection into global defense. *Annu. Rev. Plant Biol.* **64,** 839–863 (2013).
2. Gurr, S. J. & Rushton, P. J. Engineering plants with increased disease resistance: how are we going to express it? *Trends Biotechnol.* **23,** 283–290 (2005).
3. Pajerowska-Mukhtar, K. M. *et al.* The HSF-like transcription factor TBF1 is a major molecular switch for plant growth-to-defense transition. *Curr. Biol.* **22,** 103–112 (2012).
4. Xu, G. *et al.* Global translational reprogramming is a fundamental layer of immune regulation in plants. *Nature* http://dx.doi.org/10.1038/nature22371 (2017).
5. Gurr, S. J. & Rushton, P. J. Engineering plants with increased disease resistance: what are we going to express? *Trends Biotechnol.* **23,** 275–282 (2005).
6. Boller, T. & Felix, G. A renaissance of elicitors: perception of microbe-associated molecular patterns and danger signals by pattern-recognition receptors. *Annu. Rev. Plant Biol.* **60,** 379–406 (2009).
7. Schwessinger, B. *et al.* Transgenic expression of the dicotyledonous pattern recognition receptor EFR in rice leads to ligand-dependent activation of defense responses. *PLoS Pathog.* **11,** e1004809 (2015).
8. Lacombe, S. *et al.* Interfamily transfer of a plant pattern-recognition receptor confers broad-spectrum bacterial resistance. *Nature Biotechnol.* **28,** 365–369 (2010).
9. Bouwmeester, K. *et al.* The *Arabidopsis* lectin receptor kinase LecRK-I.9 enhances resistance to *Phytophthora infestans* in solanaceous plants. *Plant Biotechnol. J.* **12,** 10–16 (2014).
10. Benedetti, M. *et al.* Plant immunity triggered by engineered *in vivo* release of oligogalacturonides, damage-associated molecular patterns. *Proc. Natl Acad. Sci. USA* **112,** 5533–5538 (2015).
11. Jones, J. D. G. & Dangl, J. L. The plant immune system. *Nature* **444,** 323–329 (2006).
12. Dangl, J. L., Horvath, D. M. & Staskawicz, B. J. Pivoting the plant immune system from dissection to deployment. *Science* **341,** 746–751 (2013).
13. Kim, S. H., Qi, D., Ashfield, T., Helm, M. & Innes, R. W. Using decoys to expand the recognition specificity of a plant disease resistance protein. *Science* **351,** 684–687 (2016).
14. Chern, M. S. *et al.* Evidence for a disease-resistance pathway in rice similar to the *NPR1*-mediated signaling pathway in *Arabidopsis*. *Plant J.* **27,** 101–113 (2001).
15. Quilis, J., Peñas, G., Messeguer, J., Brugidou, C. & San Segundo, B. The *Arabidopsis AtNPR1* inversely modulates defense responses against fungal, bacterial, or viral pathogens while conferring hypersensitivity to abiotic stresses in transgenic rice. *Mol. Plant Microbe Interact.* **21,** 1215–1231 (2008).
16. Molla, K. A. *et al.* Tissue-specific expression of *Arabidopsis NPR1* gene in rice for sheath blight resistance without compromising phenotypic cost. *Plant Sci.* **250,** 105–114 (2016).
17. Huot, B., Yao, J., Montgomery, B. L. & He, S. Y. Growth-defense tradeoffs in plants: a balancing act to optimize fitness. *Mol. Plant* **7,** 1267–1287 (2014).
18. Johnson, K. C. M., Dong, O. X., Huang, Y. & Li, X. A rolling stone gathers no moss, but resistant plants must gather their moses. *Cold Spring Harb. Symp. Quant. Biol.* **77,** 259–268 (2012).
19. Rahmani, F. *et al.* Sucrose control of translation mediated by an upstream open reading frame-encoded peptide. *Plant Physiol.* **150,** 1356–1367 (2009).
20. Li, X., Clarke, J. D., Zhang, Y. & Dong, X. Activation of an EDS1-mediated *R*-gene pathway in the *snc1* mutant leads to constitutive, NPR1-independent pathogen resistance. *Mol. Plant Microbe Interact.* **14,** 1131–1139 (2001).
21. Li, Y., Yang, S., Yang, H. & Hua, J. The TIR-NB-LRR gene *SNC1* is regulated at the transcript level by multiple factors. *Mol. Plant Microbe Interact.* **20,** 1449–1456 (2007).
22. Yi, H. & Richards, E. J. A cluster of disease resistance genes in *Arabidopsis* is coordinately regulated by transcriptional activation and RNA silencing. *Plant Cell* **19,** 2929–2939 (2007).
23. Fitzgerald, H. A., Chern, M. S., Navarre, R. & Ronald, P. C. Overexpression of (*At*) NPR1 in rice leads to a BTH- and environment-induced lesion-mimic/cell death phenotype. *Mol. Plant Microbe Interact.* **17,** 140–151 (2004).
24. Lawless, C. *et al.* Upstream sequence elements direct post-transcriptional regulation of gene expression under stress conditions in yeast. *BMC Genomics* **10,** 7 (2009).
25. Calvo, S. E., Pagliarini, D. J. & Mootha, V. K. Upstream open reading frames cause widespread reduction of protein expression and are polymorphic among humans. *Proc. Natl Acad. Sci. USA* **106,** 7507–7512 (2009).

Supplementary Information is available in the online version of the paper.

Acknowledgements This study was supported by grants from National Institutes of Health 5R01 GM069594-11 and Howard Hughes Medical Institute and Gordon and Betty Moore Foundation (through grant GBMF3032) to X.D., National Natural Science Foundation of China (31371926) to M.Y., and the National Key Research and Development Program of China (2016YFD0100903) to S.W. We thank J. Motley, J. Marqués, P. Zwack and S. Zebell for comments on this manuscript.

Author Contributions G.X. and X.D. designed the research. G.X. performed the *Arabidopsis*-related experiments with help from E.Z. for fitness tests. L.L. isolated *snc1* genomic DNA. S.K. maintained *Hpa* Noco2 strain in the laboratory and helped with inoculation; M.Y., C.A. and G.X. performed and S.W. supervised the rice-related experiments. G.X. and X.D. wrote the manuscript with input from all authors.

Author Information Reprints and permissions information is available at www.nature.com/reprints. The authors declare competing financial interests: details are available in the online version of the paper. Readers are welcome to comment on the online version of the paper. Publisher's note: Springer Nature remains neutral with regard to jurisdictional claims in published maps and institutional affiliations. Correspondence and requests for materials should be addressed to X.D. (xdong@duke.edu).

Reviewer Information *Nature* thanks J. Bailey-Serres, P. Rushton and the other anonymous reviewer(s) for their contribution to the peer review of this work.

METHODS

No statistical methods were used to predetermine sample size. The experiments were not randomized. The investigators were not blinded to allocation during experiments and outcome assessment.

Plasmid construction. The 35S promoter with duplicated enhancers was amplified from pRNAi-LIC[26] and flanked with PstI and XbaI sites using primers P1/P2. The nopaline synthase (NOS) terminator was amplified from pRNAi-LIC and flanked with KpnI and EcoRI sites using primers P3/P4. Gateway cassette with LIC adaptor sequences was amplified and flanked with KpnI and AflII sites using primers P5/P6/P7 (the PCR fragment by P5/P6 was used as template for P5/P7) from pDEST375 (GenBank accession number KC614689.1). The NOS terminator, the 35S promoter, and the Gateway cassette were sequentially ligated into pCAMBIA1300 (GenBank accession number AF234296.1) via KpnI/EcoRI, PstI/XbaI, and KpnI/AflII, respectively. The resultant plasmid was used as an intermediate plasmid. The 5′ leader sequences of *TBF1* (upstream of the ATG start codon of TBF1) with WT uORFs and mutant uorfs were amplified with P8/P9 and P8/P10 from the previously published plasmids[3] carrying uORF1–uORF2–GUS and uorf1–uorf2–GUS, respectively, and cloned into the intermediate plasmid via XbaI/KpnI. The resultant plasmids were designated as pGX179 (*35S:uORFs$_{TBF1}$-Gateway-NOS*) and pGX180 (*35S:uorfs$_{TBF1}$-Gateway-NOS*). TBF1p was amplified from the *Arabidopsis* genomic DNA and flanked with HindIII/AscI using primers P11/P1, and the *TBF1* 5′ leader sequence was amplified from pGX180 and flanked with AscI/KpnI using primers P8/P13. The TBF1 promoter (P11/P12) and the *TBF1* 5′ leader sequence (P8/P13) were digested with AscI, ligated, and used as template for PCR and introduction of HindIII/KpnI using primer P11/P8. The 35S promoter in pGX179 was replaced by the TBF1 promoter to produce pGX1 (*TBF1p:uORFs$_{TBF1}$-Gateway-NOS*). The TBF1 promoter was amplified from the *Arabidopsis* genomic DNA and flanked with HindIII/SpeI using primers P14/P15 and ligated into pGX179, which was cut with HindIII/XbaI, to generate pGX181 (*TBF1p:uorfs$_{TBF1}$-Gateway-NOS*). *LUC*, *GFP$_{ER}$*, and *snc1* were amplified from pGWB235 (ref. 27), GFP–HDEL[28], and the *snc1* mutant genomic DNA, respectively. *TBF1–YFP* and *NPR1–EGFP* were fused together through PCR, cloned via ligation independent cloning[26]. EFR was amplified from U21686 (The Arabidopsis Information Resource), fused with EGFP and controlled by the 35S promoter. The 5′ leader sequence of *bZIP11* (containing uORFs$_{bZIP11}$) was amplified from the *Arabidopsis* genomic DNA with G904/G905. The start codons (ATG) for uORF2a and uORF2b in the 5′ leader sequence were mutated to CTG and TAG, respectively, to generate uorf2a$_{bZIP11}$ and uorf2b$_{bZIP11}$ by PCR using primers containing point mutations. Primer and plasmid information can be found in Supplementary Table 1.

***Arabidopsis* growth, transformation, and pathogen infection.** The *Arabidopsis Col-0* accession was used for all experiments. Plants were grown on soil (Metro Mix 360) at 22 °C with 55% relative humidity and under 12/12-h light/dark cycles for bacterial growth assay and measurements of plant radius and fresh weight, or 16/8-h light/dark cycles for seed weight and silique number measurements. The floral dip method[29] was used to generate transgenic plants. The *BGL2:GUS* reporter line[20] was used for *snc1*-related transformation. For infection, bacteria were first grown on a King's B medium plate at 28 °C for 2 days before being resuspended in 10 mM $MgCl_2$ solution for infiltration. The antibiotic selection for *Psm* ES4326 was 100 μg ml^{-1} streptomycin, for *Pst* DC3000 25 μg ml^{-1} rifampicin, and for *Pst* DC3000 *hrcC*$^{-}$ 25 μg ml^{-1} rifampicin and 30 μg ml^{-1} chloramphenicol. For spray inoculation, *Psm* ES4326 was transferred to liquid King's B with 100 μg ml^{-1} streptomycin, grown for another 8–12 h to an optical density at 600 nm ($OD_{600\,nm}$) = 0.6–1.0 and sprayed at $OD_{600\,nm}$ = 0.4 in 10 mM $MgCl_2$ with 0.02% Silwet L-77. Infected leaf samples were collected on day 0 (four biological replicates with three leaf discs each) and day 3 (eight replicates with three leaf discs each). For *Hpa* Noco2 infection, 12-day-old plants grown under 12/12-h light/dark cycles with 95% relative humidity were sprayed with 4×10^4 spores per millilitre and incubated for 7 days. Spores were collected by suspending infected plants in 1 ml of water and counted in a haemocytometer under microscopy.

Transient expression in *N. benthamiana*. *N. benthamiana* plants were grown at 22 °C under 12/12-h light/dark cycles before used for *Agrobacterium*-mediated transient expression. *Agrobacterium* GV3101 transformed with each construct was grown in Luria-Bertani broth with kanamycin (50 μg ml^{-1}), gentamycin (50 μg ml^{-1}) and rifampicin (25 μg ml^{-1}) at 28 °C overnight. Cells were resuspended in the infiltration buffer (10 mM 2-(*N*-morpholino) ethanesulfonic acid (MES), 10 mM $MgCl_2$, 200 μM acetosyringone) at $OD_{600\,nm}$ = 0.1 and incubated at room temperature for 4 h before infiltration. Activity of cytosol-synthesized firefly luciferase was detected after spraying 1 mM luciferin and displayed by chemiluminescence with pseudo-colour after transient expression in *N. benthamiana* for 2 days. Fluorescence of ER-synthesized GFP_{ER} was detected under ultraviolet light after transient expression in *N. benthamiana* for 2 days. Cell death induced by overexpression of TBF1–YFP fusion was examined by clearing with ethanol after transient expression in *N. benthamiana* for 3 days. For elf18 induction in *N. benthamiana*, the *Agrobacterium* harbouring the elf18 receptor-expressing construct (pGX664) was co-infiltrated with the *Agrobacterium* carrying the test construct at 1:1 ratio. Twenty hours later, the same leaves were infiltrated with 10 mM $MgCl_2$ (Mock) solution or 10 μM elf18 before leaf disc collection 2 h later.

Dual-luciferase assay. The $MgCl_2$ solution (10 mM), *Psm* ES4326 ($OD_{600\,nm}$ = 0.02), *Pst* DC3000 ($OD_{600\,nm}$ = 0.02), *Pst* DC3000 *hrcC*$^{-}$ ($OD_{600\,nm}$ = 0.02), elf18 (10 μM), or flg22 (10 μM) was infiltrated. Leaf discs were collected at the indicated time points. LUC and RLUC activities were measured as counts per second using a Victor3 plate reader (PerkinElmer) according to kit from Promega (E1910).

Real-time PCR. Approximately 100 mg leaf tissue was collected for total RNA extraction with TRIzol (Ambion). DNase I (Ambion) treatment was performed before reverse transcription with SuperScript III Reverse Transcriptase (Invitrogen) using oligo (dT). Real-time PCR was done using FastStart Universal SYBR Green Master (Roche). Primers used are listed in Supplementary Table 1.

Rice growth, transformation, and pathogen infection. For observation of the lesion mimic disease phenotype, rice was grown in greenhouse for 6 weeks and moved to a growth chamber for 3 weeks (12/12-h light/dark cycles, 28 °C and 90% relative humidity). For fitness tests, rice was grown during the normal rice growing season (from November 2015 to May 2016) under field conditions in Lingshui, Hainan, China (18° N latitude). *Agrobacterium*-mediated transformation into the *O. sativa* cultivar ZH11 was used to obtain transgenic rice plants[30]. For *Xoo* infection in the greenhouse (performed in 2016), rice was grown for 3 weeks from 2 February and inoculated on 23 February with data collection on 8 March. For *Xoo* infection in the field (performed in 2016), rice was grown on 10 May in the experimental stations of Huazhong Agricultural University, Wuhan, China (31° N latitude) and inoculated on 20 July with data collection on 4 August. *Xoo* strains PXO347 and PXO99 were grown on nutrient agar medium (0.1% yeast extract, 0.3% beef extract, 0.5% polypeptone, and 1% sucrose) at 28 °C for 2 days before resuspension in sterile water and dilution to $OD_{600\,nm}$ = 0.5 for inoculation. Five to ten leaves of each plant were inoculated by the leaf-clipping method at the booting (panicle development) stage[31,32]. Disease was scored by measuring the lesion length at 14 days post inoculation (d.p.i.). PCR was performed using primer rice-F and rice-R (Supplementary Table 1) for identification of At*NPR1* transgenic plants. Both PCR-positive and -negative T_1 plants were scored. For *Xoc* infection in the growth chamber (performed in 2016), rice was grown on 20 October and inoculated on 15 November, with data collection on 29 November. *Xoc* strain RH3 was grown on nutrient agar medium (0.1% yeast extract, 0.3% beef extract, 0.5% polypeptone, and 1% sucrose) at 28 °C for 2 days before resuspension in sterile water and dilution to $OD_{600\,nm}$ = 0.5 for inoculation. Five to ten leaves of each plant were inoculated by the penetration method using a needleless syringe at the tillering stage[31]. Disease was scored by measuring the lesion length at 14 d.p.i. For *M. oryzae* infection in the growth chamber (performed in 2016), rice was grown on 15 October and inoculated on 16 November, with data collection on 23 November. *M. oryzae* isolate M2 (ref. 33) was cultured on oatmeal tomato agar medium (40 g oat, 150 ml tomato juice, 20 g agar for 1 litre of culture medium) at 28 °C. Ten microlitres of the conidia suspension (5.0×10^5 spores per millilitre) containing 0.05% Tween-20 was dropped to the press-injured spots on five to ten fully expanded rice leaves and then wrapped with cellophane tape. Plants were maintained in darkness at 90% relative humidity for 1 day and were grown under 12/12-h light/dark cycles with 90% relative humidity. Disease was scored by measuring the lesion length at 7 d.p.i. For *Xoc* and *M. oryzae*, three independent transgenic lines for each construct were tested, with data from two lines shown in Fig. 3 and from the third line in the Source Data of Fig. 3. For *Xoo* infection and fitness, four independent transgenic lines for each construct were tested, with data from two lines shown in Fig. 3 and from all four lines in Extended Data Figs 7, 8 and in the Source Data.

Immunoblot. *Arabidopsis* tissue (100 mg) infected by *Psm* ES4326 ($OD_{600\,nm}$ = 0.02) was collected and lysed in 200 μl lysis buffer (50 mM Tris, pH 7.5, 150 mM NaCl, 0.1% Triton X-100, 0.2% Nonidet P-40, protease inhibitor cocktail (Roche, one tablet for 10 ml)) before centrifugation at 12,000 r.p.m. for the supernatant. The same protocol was used to extract proteins from rice infected by *Xoo* (PXO99, at $OD_{600\,nm}$ = 0.5) using a slightly different lysis buffer (50 mM Tris-HCl, pH 7.5, 150 mM NaCl, 1 mM DTT, 1 mM PMSF, 2 mM EDTA, 0.1% Triton X-100, protease inhibitor cocktail (Roche, one tablet for 10 ml)). Antibody information and the experimental conditions can be found in Supplementary Table 1.

Statistical analyses. Normal distribution was tested using a Shapiro–Wilk test. Two-sided one-way analysis of variance together with Tukey's test was used for multiple comparisons. Sample size can be found in the Source Data. Unless specifically stated, sample size *n* means biological replicates. Experiments were done three times with similar results for all the *Arabidopsis* experiments. GraphPad Prism 6 was used for all the statistical analyses.

Data availability. The authors declare that the main data supporting the findings of this study are available within the article and its Source Data files. Extra data are available from the corresponding author upon request.

26. Xu, G. *et al.* One-step, zero-background ligation-independent cloning intron-containing hairpin RNA constructs for RNAi in plants. *New Phytol*. **187,** 240–250 (2010).
27. Nakagawa, T. *et al.* Development of series of gateway binary vectors, pGWBs, for realizing efficient construction of fusion genes for plant transformation. *J. Biosci. Bioeng.* **104,** 34–41 (2007).
28. Xu, G. *et al.* Plant ERD2-like proteins function as endoplasmic reticulum luminal protein receptors and participate in programmed cell death during innate immunity. *Plant J*. **72,** 57–69 (2012).
29. Clough, S. J. & Bent, A. F. Floral dip: a simplified method for *Agrobacterium*-mediated transformation of *Arabidopsis thaliana*. *Plant J*. **16,** 735–743 (1998).
30. Lin, Y. J. & Zhang, Q. Optimising the tissue culture conditions for high efficiency transformation of indica rice. *Plant Cell Rep*. **23,** 540–547 (2005).
31. Yuan, M. *et al.* A host basal transcription factor is a key component for infection of rice by TALE-carrying bacteria. *eLife* **5,** e19605 (2016).
32. Yuan, Y. *et al.* Functional analysis of rice *NPR1*-like genes reveals that *OsNPR1/NH1* is the rice orthologue conferring disease resistance with enhanced herbivore susceptibility. *Plant Biotechnol. J.* **5,** 313–324 (2007).
33. Kang, H. *et al.* Dissection of the genetic architecture of rice resistance to the blast fungus *Magnaporthe oryzae*. *Mol. Plant Pathol.* **17,** 959–972 (2016).

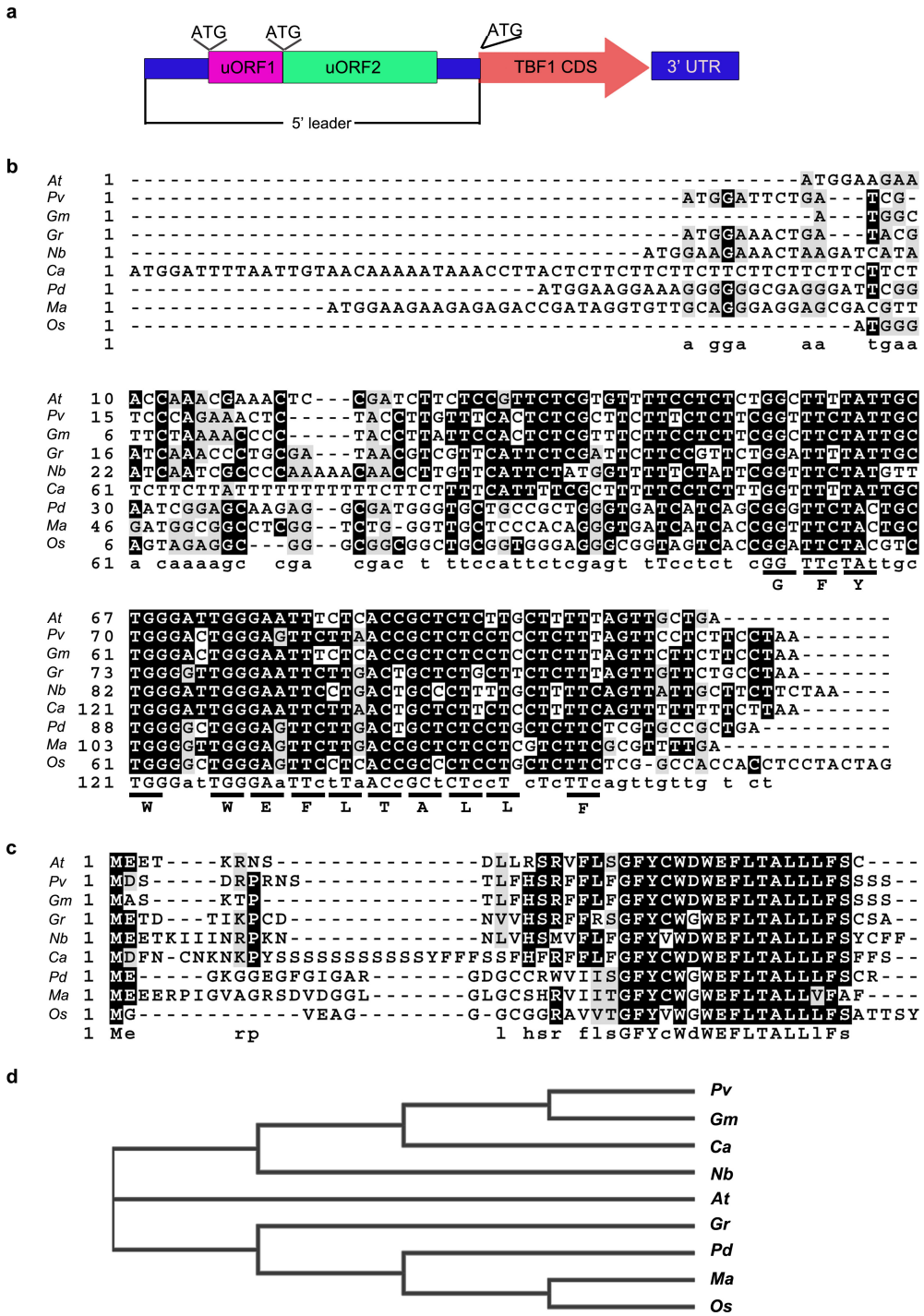

Extended Data Figure 1 | Conservation of uORF2$_{TBF1}$ nucleotide and peptide sequences in plant species. a, Schematic of *TBF1* mRNA structure. The 5′ leader sequence contains two uORFs, uORF1 and uORF2. CDS, coding sequence. **b**–**d**, Alignment of uORF2 nucleotide sequences (**b**) and alignment (**c**) and phylogeny (**d**) of uORF2 peptide sequences in different plant species. The corresponding triplets encoding the conserved amino acids among these species are underlined. Identical residues (black background), similar residues (grey background), and missing residues (dashes) were identified using Clustlw2. *At* (*Arabidopsis thaliana*; AT4G36988), *Pv* (*Phaseolus vulgaris*; XP_007155927), *Gm* (*Glycine max*; XP_006600987), *Gr* (*Gossypium raimondii*; CO115325), *Nb* (*Nicotiana benthamiana*; CK286574), *Ca* (*Cicer arietinum*; XP_004509145), *Pd* (*Phoenix dactylifera*; XP_008797266), *Ma* (*Musa acuminata* subsp. *Malaccensis*; XP_009410098), *Os* (*O. sativa*; Os09g28354).

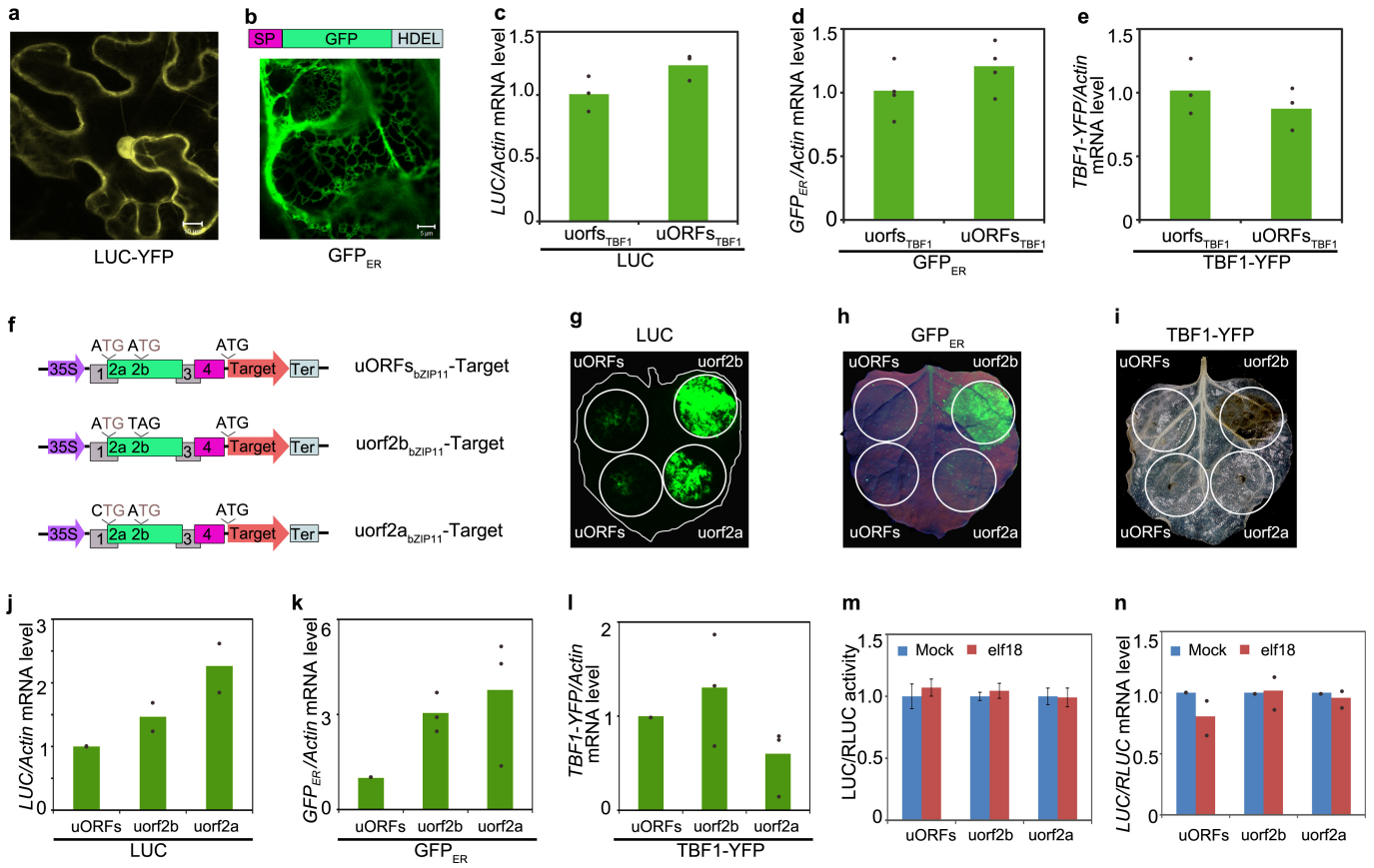

Extended Data Figure 2 | Characterization of uORFs$_{TBF1}$ and uORFs$_{bZIP11}$ in translational control. Related to Fig. 1. **a**, **b**, Subcellular localization of the LUC–YFP fusion (**a**) and GFP$_{ER}$ (**b**). SP, signal peptide from *Arabidopsis* basic chitinase; HDEL, ER retention signal. Representative of eight images. Scale bar, 10 μm. **c**–**e**, mRNA levels of *LUC* in (Fig. 1b; $n = 3$), *GFP$_{ER}$* in (Fig. 1c; $n = 4$), and *TBF1–YFP* in (Fig. 1d; $n = 3$) 2 d.p.i. before cell death was observed in plants expressing *TBF1*. **f**, Schematics of the 5′ leader sequences used in studying the translational activities of WT uORFs$_{bZIP11}$, mutant uorf2a$_{bZIP11}$ (ATG to CTG), or uorf2b$_{bZIP11}$ (ATG to TAG). **g**–**i**, uORFs$_{bZIP11}$-mediated translational control of cytosol-synthesized LUC (**g**; chemiluminescence with pseudo-colour); ER-synthesized GFP$_{ER}$ (**h**; fluorescence under ultraviolet light); and cell death induced by overexpression of TBF1–YFP fusion (**i**; cleared using ethanol) after transient expression in *N. benthamiana* for 2 days (**g**, **h**) and 3 days (**i**), respectively. Representative of four images. **j**–**l**, mRNA levels of *LUC* in (**g**; $n = 2$ experiments with three technical replicates), *GFP$_{ER}$* in (**h**; $n = 3$ experiments with three technical replicates), and *TBF1–YFP* in (**i**; $n = 3$ experiments with three technical replicates). **m**, Translational efficiency changes in LUC controlled by the 5′ leader sequence containing WT uORFs$_{bZIP11}$, mutant uorf2a$_{bZIP11}$, or uorf2b$_{bZIP11}$ in response to elf18 in *N. benthamiana*. Mean of the LUC/RLUC activity ratios ($n = 12$). **n**, *LUC*/*RLUC* mRNA changes in **m**. Mean of *LUC*/*RLUC* mRNA normalized to Mock from two experiments with three technical replicates. Bar with solid circles, mean with individual biological replicates.

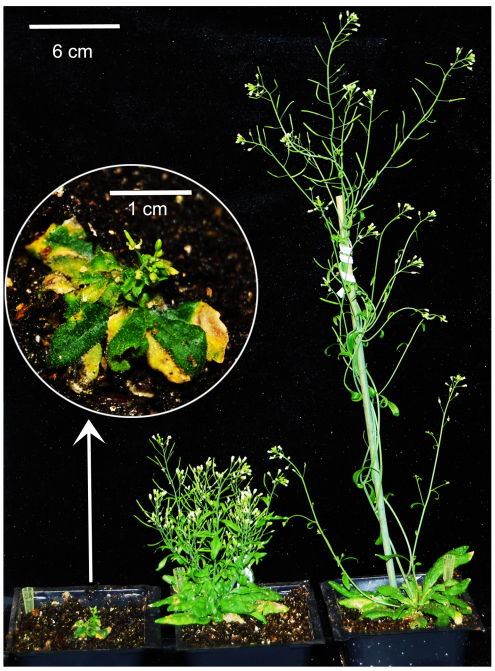

Genotype (T_1)	Type I	Type II	Type III	Total
35S:uorfs$_{TBF1}$-snc1	23	0	0	23 (a)
35S:uORFs$_{TBF1}$-snc1	25	3	14	42 (b)
TBF1p:uorfs$_{TBF1}$-snc1	6	9	8	23 (c)
TBF1p:uORFs$_{TBF1}$-snc1	0	10	22	32 (d)

Extended Data Figure 3 | Three developmental phenotypes observed in primary *Arabidopsis* transformants expressing *snc1*. The three developmental phenotypes observed in T_1 (that is, the first generation) *Arabidopsis* transgenic lines carrying *35S:uorfs$_{TBF1}$-snc1*, *35S:uORFs$_{TBF1}$-snc1*, *TBF1p:uorfs$_{TBF1}$-snc1*, and *TBF1p:uORFs$_{TBF1}$-snc1* (above). Representative of five images. Fisher's exact test was used for the pairwise statistical analysis (below). Different letters in 'Total' indicate significant differences between type III versus type I + type II ($P < 0.01$).

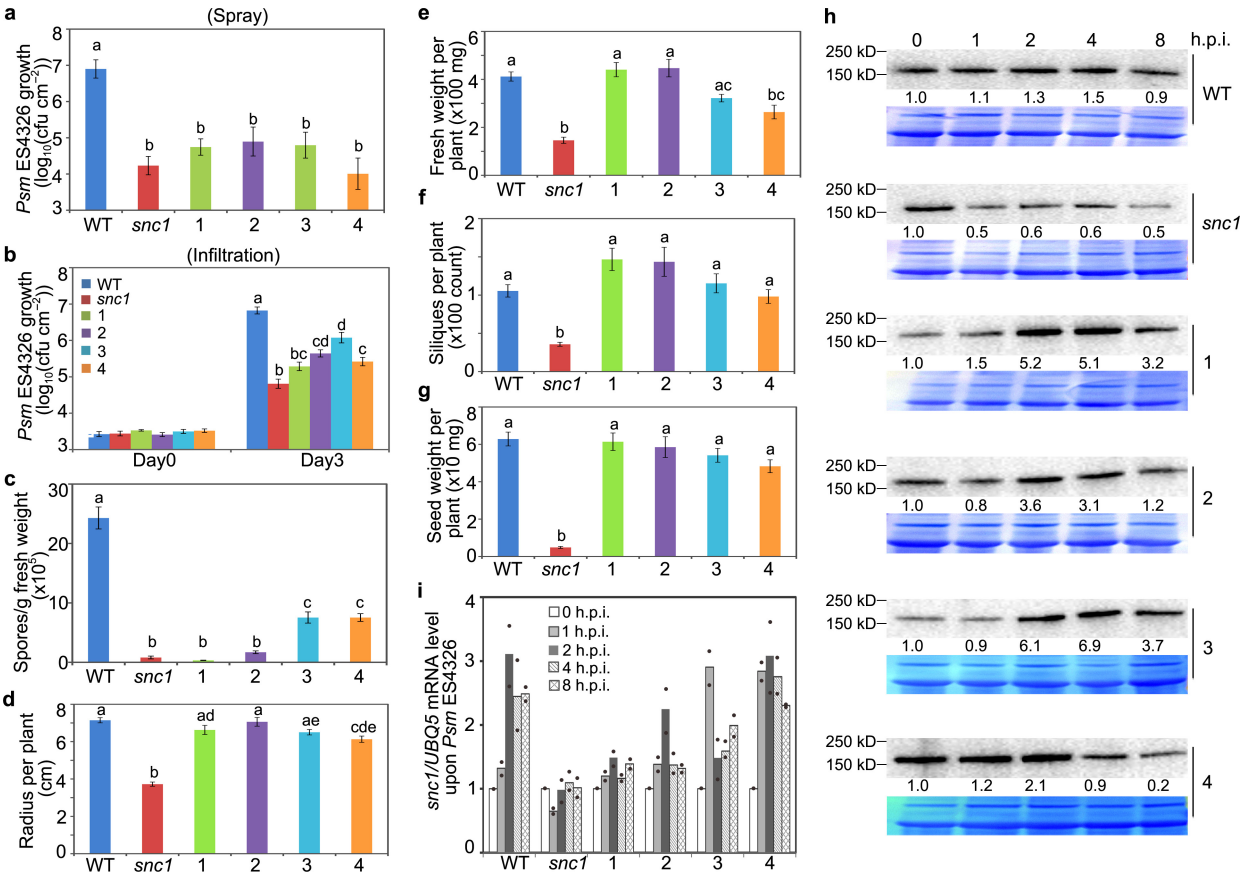

Extended Data Figure 4 | Effects of controlling transcription and translation of *snc1* on defence and fitness in *Arabidopsis*. Related to Fig. 2. **a**, **b**, *Psm* ES4326 growth in WT, *snc1*, transgenic line numbers 1–4 after inoculation by spray (**a**) or infiltration (**b**). Mean ± s.e.m. **c**, *Hpa* Noco2 growth as measured by spore counts 7 d.p.i. Mean ± s.e.m. **d**–**g**, Analyses of plant radius (**d**), fresh weight (**e**), silique number (**f**), and total seed weight (**g**). Mean ± s.e.m. **h**, **i**, Relative levels of *Psm* ES4326-induced snc1 protein (**h**; numbers below immunoblots; see Supplementary Fig. 1 for gel source data) and mRNA (**i**; mean from two experiments with three technical replicates). Solid circles, individual biological replicates. Numbers 1–4, four independent transgenic lines carrying *TBF1p:uORFs*$_{TBF1}$*-snc1* with 1 and 2 shown in Fig. 2. h.p.i., hours after *Psm* ES4326 infection; CBB, Coomassie brilliant blue. See Source Data for sample size (*n*). Different letters above bars indicate significant differences ($P < 0.05$).

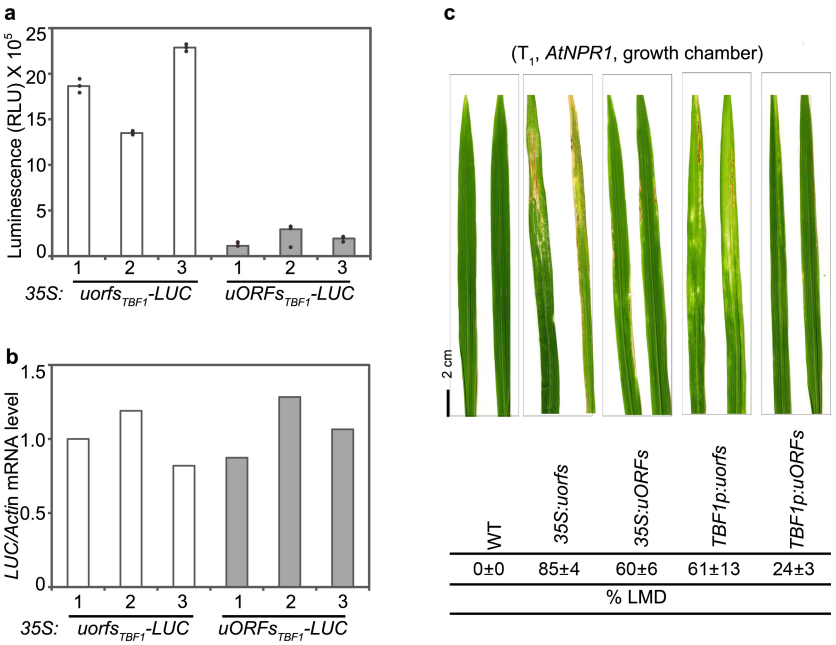

Extended Data Figure 5 | Functionality of uORFs$_{TBF1}$ in rice. **a**, **b**, LUC activity (**a**) and mRNA levels (**b**) in three independent primary transgenic rice lines (called 'T_0' in rice research) carrying *35S:uorfs$_{TBF1}$-LUC* and *35S:uORFs$_{TBF1}$-LUC*. Mean of LUC activities (RLU, relative light unit) of three biological replicates. Solid circles, individual biological replicates; and mean of *LUC* mRNA levels of three technical replicates after normalization to the *35S:uorfs$_{TBF1}$-LUC* line 1. **c**, Representative lesion mimic disease (LMD) phenotypes (above) and percentage of At*NPR1*-transgenic rice plants showing lesion mimic disease in the second generation (T_1) grown in the growth chamber (below).

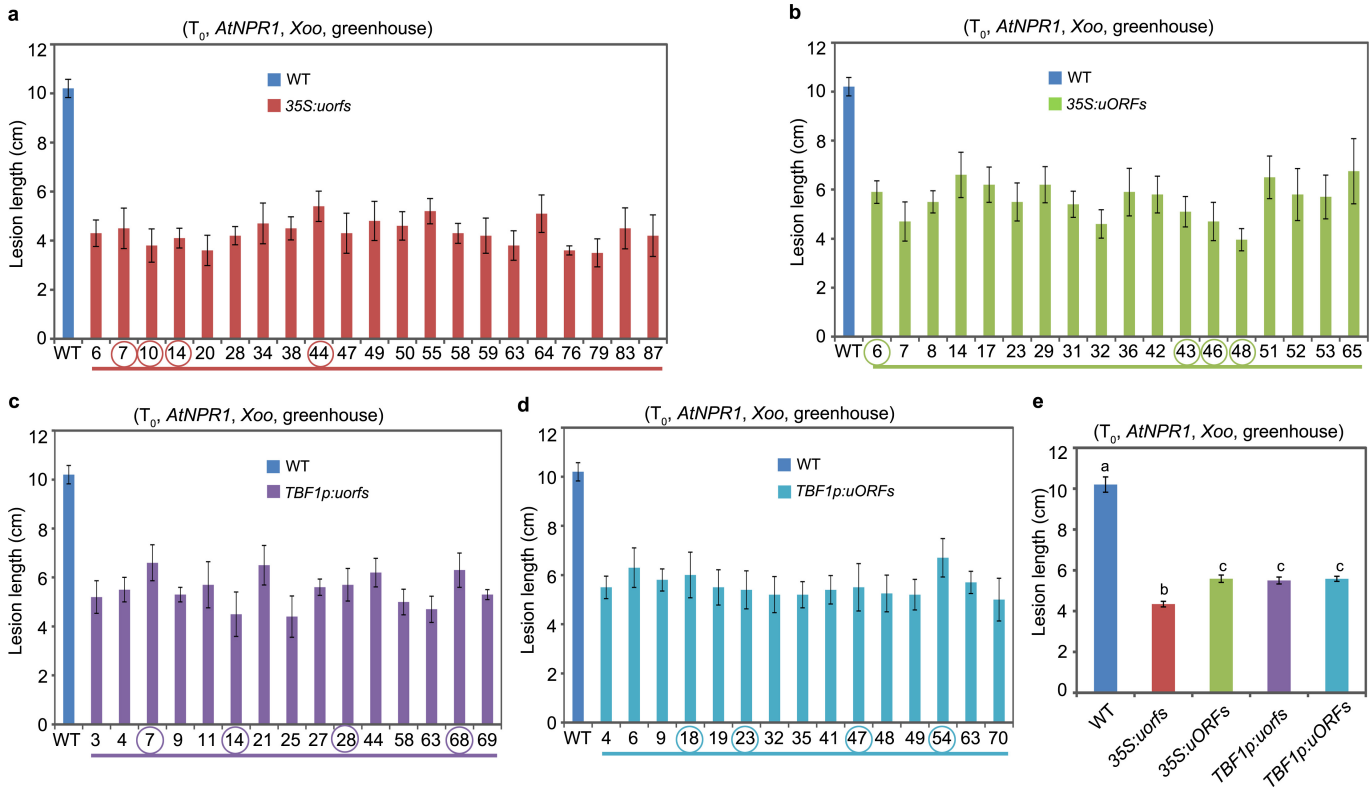

Extended Data Figure 6 | Effects of controlling transcription and translation of At*NPR1* on defence in T_0 rice. Related to Fig. 3. **a**–**d**, Lesion length measurements after infection by *Xoo* strain PXO347 in primary transformants (T_0) for *35S:uorfs*$_{TBF1}$-At*NPR1* (**a**), *35S:uORFs*$_{TBF1}$-At*NPR1* (**b**), *TBF1p:uorfs*$_{TBF1}$-At*NPR1* (**c**), and *TBF1p:uORFs*$_{TBF1}$-At*NPR1* (**d**). Lines further analysed in T_1 and T_2 are circled. **e**, Average leaf lesion lengths. WT, recipient *O. sativa* cultivar ZH11. Mean ± s.e.m. Different letters above bars indicate significant differences ($P < 0.05$). See Source Data for sample size (n).

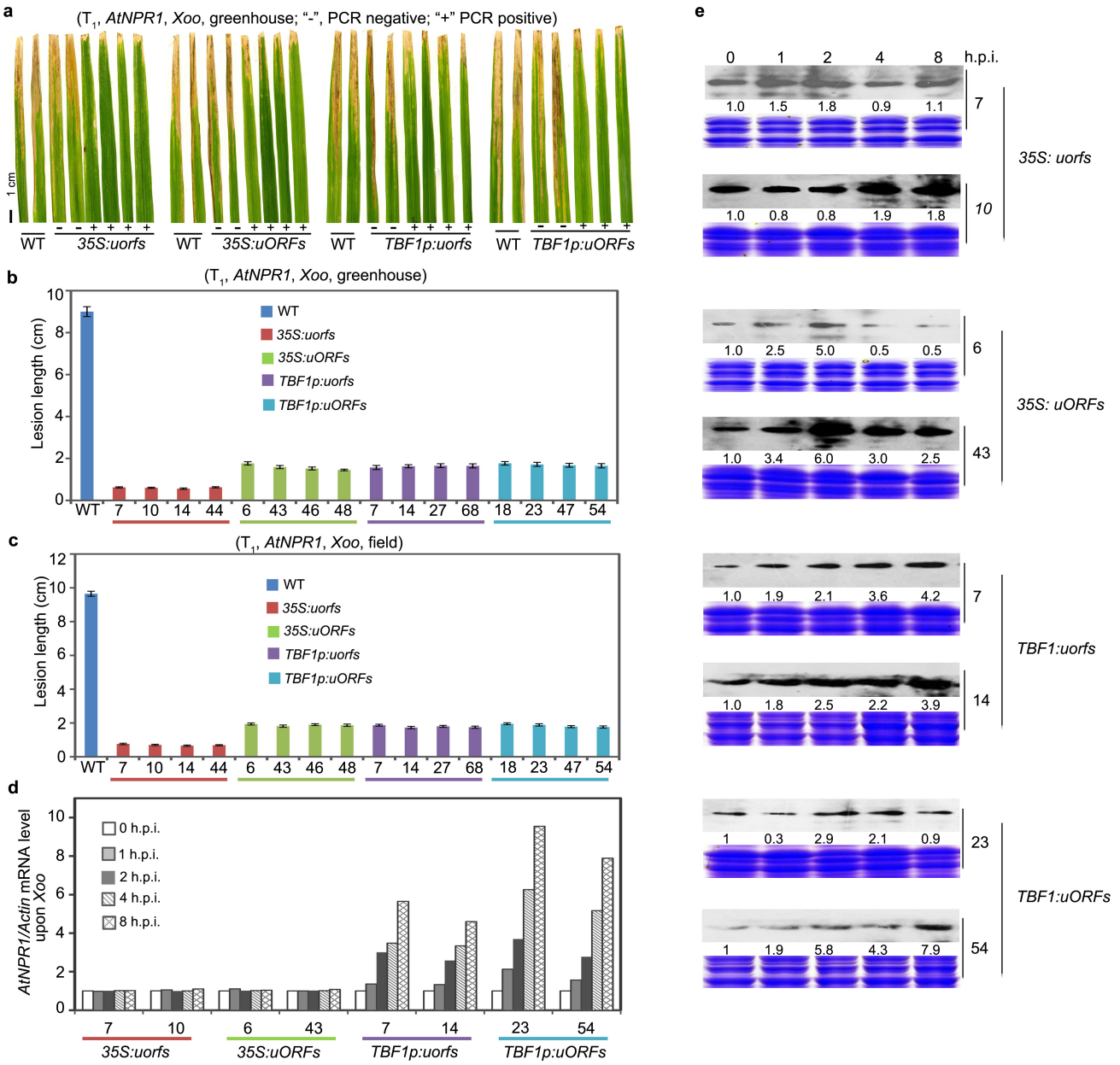

Extended Data Figure 7 | Effects of controlling transcription and translation of At*NPR1* on defence in T_1 rice. Related to Fig. 3. **a**, **b**, Representative symptoms observed in T_1 At*NPR1*-transgenic rice plants grown in the greenhouse (**a**) after *Xoo* inoculation and corresponding leaf lesion length measurements (**b**). PCR was performed to detect the presence (+) or the absence (−) of the transgene gene. **c**, Quantification of leaf lesion length of four lines for *Xoo* inoculation in field-grown T_1 At*NPR1*-transgenic rice plants. Mean ± s.e.m. See Source Data for sample size (*n*). Different letters above bars indicate significant differences ($P < 0.05$). **d**, **e**, Relative levels of At*NPR1* mRNA (**d**) and protein (**e**; numbers below immunoblots; see Supplementary Fig. 1 for gel source data) in response to *Xoo* infection. Mean of At*NPR1* mRNA levels of three technical replicates after normalization to 0 h.p.i. (**d**). Solid circles, individual biological replicates.

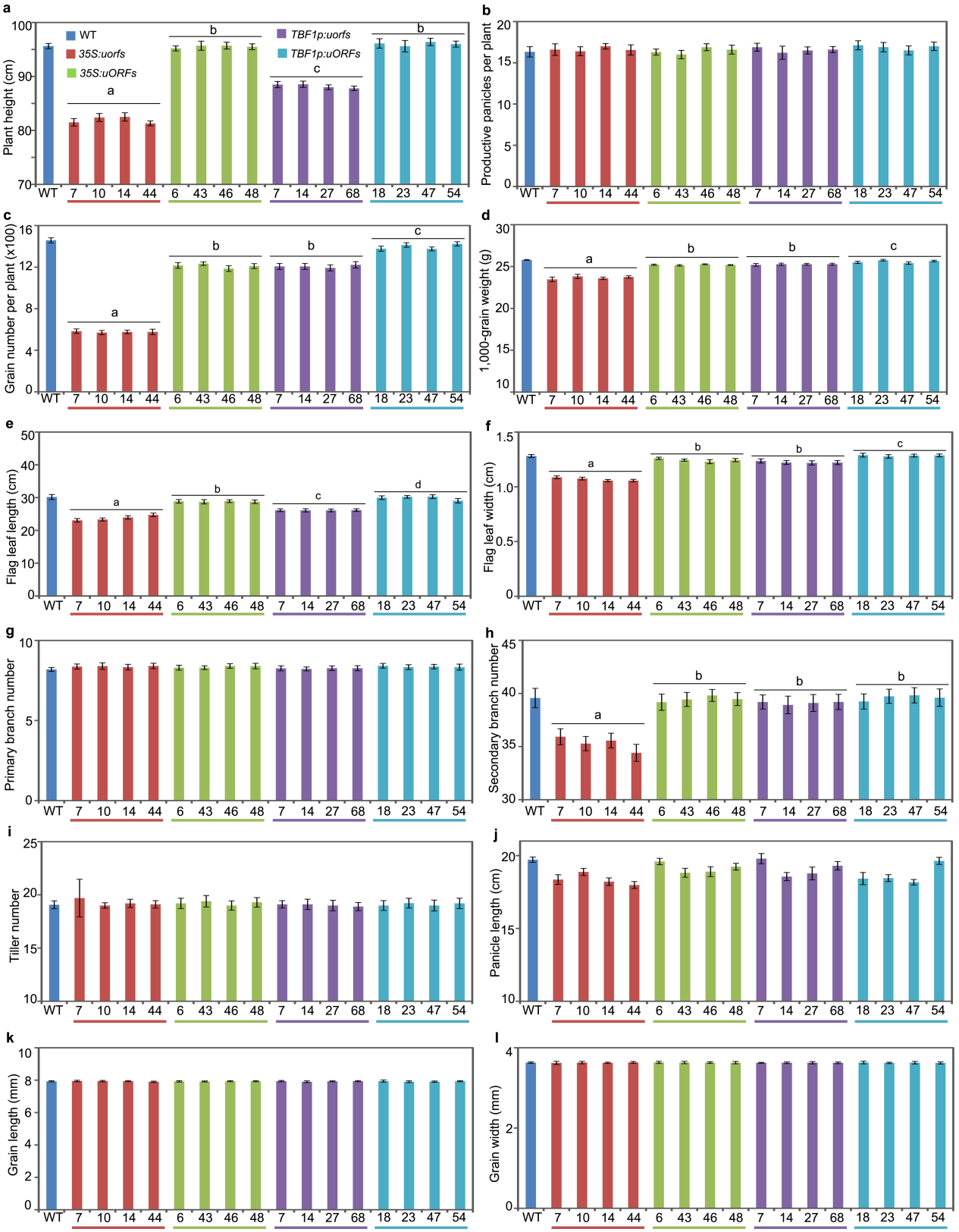

Extended Data Figure 8 | Effects of controlling transcription and translation of At*NPR1* on fitness in T_1 rice under field conditions. Related to Fig. 3. Mean ± s.e.m. See Source Data for sample size (*n*). Different letters above bars indicate significant differences among constructs ($P < 0.05$).